Assessment of nutrient remobilization through structural changes of palisade and spongy parenchyma in oilseed rape leaves during senescence

Clément Sorin, Maja Musse, Francois Mariette, Alain Bouchereau, Laurent Leport

Assessment of nutrient remobilization through structural changes of palisade and spongy parenchyma in oilseed rape leaves during senescence

Clément Sorin, Maja Musse*, François Mariette, Alain Bouchereau, Laurent Leport

Institut National de Recherche en Sciences et Technologies pour l'Environnement et l'Agriculture, Food Process Engineering Research Unit, F-35044 Rennes cedex, France (C.S, M.M, F.M.); Université Européenne de Bretagne, 5 Boulevard Laënnec, 35000 Rennes, France (C.S., M.M, A.B., F.M., L.L.); INRA, UMR 1349, Institute for Genetics, Environment and Plant Protection (IGEPP), UMR INRA-Agrocampus Ouest-Université de Rennes 1, 35653 Le Rheu cedex, France (C.S., A.B., L.L.)

Corresponding author: Maja MUSSE

Telephone : +33223482179

E-mail : maja.musse@irstea.fr

Main conclusion: Differential palisade and spongy parenchyma structural changes in oilseed rape leaf were demonstrated. These dismantling processes were linked to early senescence events and associated to remobilization processes.

ABSTRACT

During leaf senescence, an ordered cell dismantling process allows efficient nutrient remobilization. However, in *Brassica napus* plants, an important amount of nitrogen (N) in fallen leaves is associated with low N remobilization efficiency. The leaf is a complex organ mainly constituted of palisade and spongy parenchyma characterized by different structures and functions concerning water relations and carbon fixation. The aim of the present study was to demonstrate a specific structural evolution of these parenchyma throughout natural senescence in *Brassica napus*, probably linked to differential nutrient remobilization processes. The study was performed on 340 leaves from 32 plants during an 8-week development period under controlled growing conditions. Water distribution and status at the cellular level were investigated by low field proton Nuclear Magnetic Resonance (NMR), while light and electron microscopy were used to observe cell and plast structure. Physiological parameters were determined on all leaves studied and used as indicators of leaf development and remobilization progress. The results revealed a process of hydration and cell enlargement of leaf tissues associated with senescence. Wide variations were observed in the palisade parenchyma while spongy cells changed only very slightly. The major new functional information revealed was the link between the early senescence events and specific tissue dismantling processes.

Key words: leaf senescence, microscopy, NMR relaxometry, oilseed rape, palisade

INTRODUCTION

A leaf goes through different phases during its development, the last being senescence. Senescence is a highly regulated complex process that leads to the death of the tissue. This process has been shown to involve three phases (Nooden et al. 1997). The first phase is regulated by hormones and is characterized by transduction of the senescence signal (from environmental or internal factors) that leads to activation of key genes. The second phase is a degenerative phase corresponding to the disassembly and remobilization of cell components. Remobilization during that phase allows recycling cell nutrients from senescing tissues to growing organs. Finally, the terminal phase corresponds to disorganization of the nucleus, degeneration of the tonoplast and distortion of the cell wall leading to the cell death. Mitochondria remain active until the latest stage of senescence (Sakamoto 2006). All these events are programmed in order to allow maximal carbon (C) and nitrogen (N) remobilization in correspondence with sink demand. For crop species, the ability of the plant to remobilize nutrients highly impacts seed yield, especially in the current context of fertilizer input reduction. For instance, oilseed rape crop is known to have suboptimal N use efficiency partly due to low leaf organic N recycling performance and inherent important N residual amount in fallen leaves. As nitrogen fertilization has a major impact on oilseed rape production costs and environment quality, low N remobilization efficiency (NRE) has negative economical and agro-ecological consequences. Improving oilseed rape NRE should be a breeding challenge and would therefore necessitate a better understanding of senescence associated nutrient allocation and partitioning processes in leaves especially at the cell structure and organization levels were organites and macromolecules constitute predominant sources for metabolite recycling and sink feeding.

A leaf is constituted of the palisade and the spongy parenchyma crossed by vascular tissues and surrounded by two epidermises. In *Brassica napus*, the palisade parenchyma consists of regular shaped cells organized in layers whereas the spongy parenchyma, presenting large intercellular spaces, is less well organized (Castro-Diez et al. 2000). The principal leaf functions are photosynthesis, photorespiration and transpiration. Even if there is no experimental data supporting that, it is currently accepted that photosynthesis is mainly performed by palisade tissue (Nardini et al. 2010) whereas the spongy tissue is known to be involved in gas exchange. Moreover, it has been shown in *Acer hippocastanum* (horse chestnut) with abaxial position of stomata that the spongy tissue has a major role in the homeostasis of the leaf hydraulic status (Nardini et al. 2010). Although the leaf has often been studied as a homogeneous organ the structural and functional differences described above may suggest different patterns of evolution during development and senescence. It might be expected that palisade and spongy tissues evolve differently in terms of metabolism during senescence possibly leading to different contributions to remobilization process. The question of differential evolution of the palisade and spongy parenchyma during leaf development has not been addressed to date in the literature. The only differential response between leaf parenchyma were revealed by microscopy in plant under water (Bacelar et al. 2006; Martinez et al. 2007) and ozone stresses (Bohler et al. 2013).

As already stated structural modifications due to macromolecules dismantling and recycling in senescing leaves are at the origin of cell compartment disruption, dry matter reallocation and probably water redistribution between compartments. Low field proton Nuclear Magnetic Resonance (NMR) has been used for investigation of cell water compartmentalization in various plant organs (Hills and Remigereau 1997; McCain 1995; van der Weerd et al. 2001). The technique allows measurement of relaxation signals that for highly

hydrated plant tissues originate mainly from water. In the case of compartmentalized systems characterized by slow diffusion exchange of water molecules between compartments, relaxation times have a multi-exponential character due to differences in physical and chemical properties of water in different compartments. The relaxation signal is therefore used to study changes in water status and distribution. In most studies, transverse relaxation time (T2) has been used rather than longitudinal relaxation time (T1) as it is more sensitive to variations in water properties occurring in plant tissues. The multi-exponential T2 has mainly been interpreted at a cell level to assign different signal components to principal cell compartments while assuming homogeneity of cells in the sample being examined (Snaar and Van As 1992b). This model was developed for fleshy fruit (Snaar and Van As 1992a) and vegetable parenchyma (Hills and Remigereau 1997). It has also been used for leaf tissues from different plants (Capitani et al. 2009; Colire et al. 1988). Another approach was used by Qiao *et al*. (2006) who considered only heterogeneity of the sample at the tissue level. Musse *et al*. (2013), investigating leaf senescence of *Brassica napus*, recently drew attention to the fact that both cell compartmentalization and tissue heterogeneity have to be taken into account in the interpretation of the NMR signal. The NMR signal of leaves was shown to be sensitive to the senescence stage and all signal components to be affected by it. The principal signal changes concerned the vacuole-related component that separated into two components in senescing leaves. An interpretation was proposed associating these changes with a process of cell enlargement and hydration, probably linked to remobilization processes.

The focus of the present study was on changes occurring in vacuole properties, the major place of macromolecules degradation during remobilization, and plast structures that constitute the main N reserve of the leaf, during leaf senescence. NMR measurements and an extended microscopy study were performed to observe changes at both cellular and tissue levels. Light microscopy was used for the quantification of tissue thickness and vacuolar volume, whereas plasts and cell walls were investigated using electronic microscopy. The design of the experiment allowed investigation of natural leaf senescence in a large number of plants grown under controlled conditions through an eight-week kinetics study. This design made it possible to compare different developmental scales commonly used to describe senescence (i.e. leaf rank, leaf age and physiological markers). The output of the study was to demonstrate a differential structural and probably functional evolution linked to nutrient remobilization processes of palisade and spongy parenchyma cells in naturally senescent leaves of *Brassica napus*.

MATERIALS AND METHODS

Plant material

About 10 seeds (homogenous weight) of oilseed rape, *Brassica napus* L., genotype Tenor, were sown in individual containers filled with a growing medium (FALIENOR 9226-6F2) containing 65% light peat, 20% dark peat and 15% perlite. Four sowings (series S-1, S-2, S-3, and S-4) were undertaken at one-week intervals. The 8 most homogenous three-week-old seedlings of each series were individually planted into four-liter pots filled with the same growing medium and grown in a growth cabinet for five (t1) to twelve (t8) weeks. The 32 plants used for this experiment were watered throughout the growing period, with a fertilizing solution

(Liquoplant bleu) used at 3‰ and irrigation was adjusted to the evaporation-transpiration rate of the pots. The growth cabinet conditions were 14hr daylight (at 200 µmol photons m^{-2} s^{-1}) and 10hr dark (relative humidity: 75/90%; temperature: 20/18°C).

Chlorophyll content

Before sampling, relative chlorophyll content per unit of leaf area was determined using a non-destructive chlorophyll meter SPAD (Soil Plant Analysis Development; Minolta, model SPAD-502). Chlorophyll content of each leaf was estimated as an average value of 6 independent measurements.

Sampling

For all series, one plant was taken each week for 8 weeks (week1 to week 8) and all the leaves for each plant were numbered according to their rank (L-1 for the first leaf after the cotyledon).

Six to ten leaf discs of 8 mm in diameter were cut from the limb tissue for the NMR measurements to sample similar tissue weights. In order to obtain homogeneous tissues, discs were taken from each side of the central vein as close as possible to the vein and avoiding lateral nervures. Discs were then placed in NMR tubes which were closed with a 2-cm long Teflon cap to avoid water loss during measurements. Leaf discs were also collected for microscopy studies from selected plants and leaf ranks,. The rest of the leaf limb was frozen in liquid nitrogen and kept at -20°C to be subsequently ground and freeze-dried for starch quantification.

For microscopy studies, mesophyll tissues were collected from series 4 (S-4) plants, from three leaves (leaf ranks 4, 6, and 8) at three times (weeks 3, 4, and 5). Five bands 3-millimeters wide and 1-centimeter long were taken perpendicularly to the central vein. In order to confirm our vacuolar volume approximation, in the first plant five bands were also collected alongside the central vein. After sampling, the fixative solution (phosphate buffer 0.1 mol. L^{-1} p H 7.4 (PB), 3% (w/v) glutaraldehyde) was infiltrated into the leaf tissues using 10 cycles of depressurization with a vacuum pump (5 min of low pressure in each cycle). Samples were returned to the same fixative solution for 24 h at 4°C and then were washed in PB and dehydrated in a graded series of increasing concentrations of ethanol (50, 70, 90 and 100% v/v). Samples were kept in pure ethanol for 12 h at 4°C.

Starch quantification

Starch was extracted from 30 mg dry weight of freeze-dried leaf limb tissue using 1 mL phosphate buffer (0.2 mol. L^{-1}, pH 6.5) for 20 min at 95°C. The supernatant was collected after centrifugation at 15,000 x g for 5 min at 4°C. The extraction step was repeated twice and the supernatants were pooled. Measurements were performed three times for each sample (following the manufacturer's recommendations (Sigma, # STA20)) after hydrolysis by α-amylase and amyloglucosidase. Starch content was expressed in glucose equivalent after subtraction of free glucose content.

Water content

Water content (WC) was measured on all leaf discs sampled for NMR relaxometry by weighing before (fresh weight) and after drying (dry weight) in an oven at 103°C for 16h. WC was expressed as percentage of fresh weight.

NMR Relaxometry

NMR Relaxometry measurements were performed with a 20 MHz spectrometer (Minispec PC-120, Bruker, Karlsruhe, Germany) equipped with a thermostatted probe. The temperature was set at 18°C. T2 was measured using the combined FID-CPMG sequence.

The FID signal was acquired from 11 µs to 70 µs at a sampling decay of 0.4 µs. For the CPMG measurements, the 90°-180° pulse spacing was 0.1 ms and the signal of a single point at the echo maximum was acquired. Data were averaged over 64 acquisitions. The number of successive echoes recorded was adjusted for each sample according to its T2. The recycle delay for each sample was adjusted after measurement of the T1 with a fast-saturation-recovery sequence. The total time of acquisition of data for T2 (including spectrometer adjustments and T1 measurement) was about 10 min per sample.

Fitting was performed in two steps: first T2 relaxation curves from the CPMG data only were fitted by Scilab software according to the MEM (Mariette et al., 1996), which provides a continuous distribution of relaxation components without any assumption concerning their number. In this representation, the peaks of the distribution are centered at the corresponding most probable T2 values, while peak areas correspond to the intensity of the T2 components. Then complete T2 relaxation curves obtained by the combined FID-CPMG sequence were analyzed using the Levenberg-Marquardt algorithm which allows a discrete solution for the fitting curve according to the equation:

$$I(t) = I_1 \exp(-t / T_{21})^2 + \sum_{i=2} I_{0i} \exp(-t / T_{2i}) + offset \qquad \text{Eq. 1}$$

where I_{0i} is the intensity of the i_{th} exponential at the equilibrium state and $T2_i$ the characteristic transverse relaxation time for the i_{th} exponential. The number of terms that best described the relaxation curve was determined by examining MEM relaxation curves. Intensity was expressed through the specific leaf water weight of the i^{th} signal component expressed in g m^{-2} (LWW). The specific LWW of each component was calculated according to the equation:

$$LWW_i = \frac{I_{R0i}\, x\, m_w}{A} \qquad \text{Eq. 2}$$

where *mw* is the water mass of the leaf disc use for NMR (in g), A the leaf disc area (in m^2) and I_{R0i} the relative intensity of the i_{th} signal component expressed as a percentage of the total CPMG intensity.

Electron and light microscopy

Sample preparation and micrograph acquisition

For light microscopy, samples stored in pure ethanol were progressively included in an acrilyc resin (LRWhite) using a graded series of increasing concentrations of resin solubilized in ethanol (20, 40, 60, 80, and

100% v/v). Polymerisation was performed at 55°C over 4 days. Thin sections (1 µm) were cut with an ultramicrotome (LEICA UC7) and stained with toluidine blue before they were observed with a NIKON Eclipse 80i microscope.

For transmission electron microscopy analysis (TEM), ethanol in samples was replaced by propylene oxide by two baths (50 and 100% v/v). Then the propylene oxide was replaced by an epoxy resin (EPON) using the same method (50 and 100% v/v) and the sample was kept for one night at 4°C in an EPON solution. Polymerisation was performed over 1 day at 55°C and 60H at 72°C. Ultra-thin sections (60 nm) were then cut with an ultramicrotome (LEICA RM 2165),and placed on grids post-stained for 60 min with uranyl acetate. The ultra-thin sections were then examined with a JEOL JEM 1230 transmission electron microscope with an accelerating voltage of 80 kV

Vacuole volume measurement

The area (A) of each cell from both parenchyma was measured using image J software. The width (W) of each cell was also measured and the results from samples taken perpendicularly or parallel to the central vein of the same leaves, were compared. No difference was observed between the two types of sample, allowing us to estimate the vacuole volume of each cell by multiplying A by W.

Data analyses

All calculations were performed using the software package Rstudio. In order to detect significant differences ($P<0.05$) between different leaf ranks, and between different weeks of sampling, one way analysis of variance test (ANOVA) was applied to all measurements. The multiple range LSD test was used to compare means of the series. Correlations were revealed through Pearson's rank correlation coefficient analysis.

RESULTS

Physiological characterization of leaf development

Leaf development was characterized through chlorophyll and starch content, water content and dry weight measurements (Fig. 1). In order to compare leaf pattern of evolution according to the position in the canopy and to time, two approaches were used to present the results:

(i) All leaves were followed during the eight-week measurement period. The eighth rank leaf (LR-8) was chosen for presentation in Fig. 1 (a, b) because it was present on the plant during the whole measurement period (from eight weeks to fifteen weeks).

(ii) All leaves from one plant were analyzed at one measurement time (b, d). The results presented correspond to the ten-week-old plant (third week of measurement period).

Fig. 1a shows that the chlorophyll content was at its maximum until the sixth week and then decreased to the end of the measurement period. The amount of starch increased until the fifth week of measurement and then started to decrease with ageing and destruction of the photosynthetic pigment. The water content was about 85% of fresh weight in young leaves (Fig. 1c) and increased during the last three weeks. Dry weight was constant until the sixth week and then decreased slightly. The results of fresh weight measurement (Supplementary data 1) showed that the increase in water content observed in old leaves was due not only to the decrease in dry weight but also to an increase in the amount of water.

Similar patterns were observed while comparing physiological parameters corresponding to different leaf ranks from the same plant at a given time (Fig. 1b, d) to those from a leaf over eight weeks (Fig. 1a, c). This demonstrated that analyzing leaves for the parameters measured in the present study throughout the canopy from old to young leaves can be considered equivalent to studying one leaf during its development.

NMR characterization of leaf development

Changes in NMR signal were followed throughout leaf development. Fig. 2 presents a continuous distribution of transverse relaxation times obtained by the maximum entropy method (MEM) calculated from the separate CPMG (Carr Purcell Meiboom Gill) data from different leaves. The dotted line represents MEM results for the selected leaf (LR-8) obtained at four different times in the eight-week measurement period. The solid line shows the results for four leaves (LR-10, LR-7, LR-5, LR-3) from one plant at one measurement time (third week). The NMR signal for *Brassica napus* leaves is characterized by four or five components, depending on leaf age (Fig. 2), the first component corresponding to the solid state protons (not represented in Fig.2) and the others to the liquid fraction (Musse et al. 2013). The longest T2 component attributed to the vacuole (Musse et al. 2013; Van As 2007) represented more than 75% of the leaf water. The T2 of this component increased with time and started to split into two components in mature leaves (Fig.2b). For senescent leaves, two separate vacuolar components were observed (Fig.2c) for which T2 values increased until the end of the measurement period (Fig.2d). As for the physiological parameters, Fig. 2 shows that the evolution of transverse relaxation time distributions was the same when monitoring one leaf during several weeks and when analyzing leaves throughout the plant axis from old to young leaves at one measurement time.

The leaf rank for which the longest T2 component observed in young leaves separated into two components is represented in Fig. 3. The emergence of the new component is from here on referred to as “the split”. Both our former study (Musse et al. 2013) and the present results showed that this split was linked to the developmental process of the leaf. Between week 2 and week 7, the leaf rank at which the split occurred increased by one rank each week (Fig. 3). During the eight-week measurement period, the number of leaves in which the split occurred represented a constant ratio of 40 - 50% of all the expanded leaves of the plant.

The results presented in Figs. 2 and 3 show that it was possible to use the split to target leaves at the same developmental stage. In this aim, tag zero was assigned to leaves in which the split had occurred, the subsequent leaf rank was numbered 1, etc. According to this scale, the older the leaf was, the higher its tag, while negative tags represented young leaves. This NMR split scale made it possible to average values from data obtained in leaves at different measurement weeks and from different leaf ranks. These results took into account all 340 leaves from the 32 plants used in this study, giving an overview of leaf development from young to very senescent leaves. The NMR split scale is used in the subsequent Figures.

The discrete solutions for the complete decay curve (FID+CPMG) obtained by the Levenberg-Marquardt algorithm agreed to a great extent with the MEM results of the separate CPMG curve. In addition, the FID provided access to a fast-relaxing component linked to the solid phase protons, with T2 of a few tens of microseconds and 2-5% of total signal intensity. Component 1 was not further analyzed but the correlation between its intensity and dry weight (Supplementary data 2) may be valuable in future studies to determine leaf age as the dry weight decreases during senescence (Fig. 1).

For the liquid fraction components, Fig. 4 shows the T2 value and relative intensity of the NMR signal (components 2 to 5) expressed in leaf water weight per leaf area during leaf development obtained by the Levenberg-Marquardt algorithm. The T2 of component 2 (Fig. 4a) remained at around 2 ms from the youngest leaves to two ranks before the split occurred (tag -7 to tag -2, according to the split scale). It then decreased progressively until tag +4 and component 2 finally disappeared in older leaves. The T2 of component 3 was relatively stable, at around 20 ms for young leaves (tag -7 to tag -1) and 16 ms for older leaves (tag +1 to tag +7). The T2 of component 4 (Fig. 4b) was around 100ms for the youngest leaves (tag -7) and progressively reached 200 ms at tag -1. After the split, the two components (4 and 5) had different pattern of evolutions, component 4 increased slightly up to 235 ms (tag +7), while the T2 of component 5 first increased steadily to 400 ms until the tag +5 and then strongly to 800 ms until tag +7.

Fig. 4c shows the relative signal intensity expressed in leaf water weight per leaf area (LWW_i) in order to present the amount of water associated with each component. The LWW_2 remained stable until the disappearance of component 2 (tag +5). The amount of water associated with component 3 increased slightly during leaf development from 40 g/m^2 (tag -7) to more than 50 g/m^2 in the oldest leaves. LWW_4 was about 220 g/m^2 before the split. At the first appearance of component 5, LWW5 was 180 g/m^2 whereas LWW4 was around 100 g/m^2. It remained around this value after the split whereas LWW_5 increased markedly to 440 g/m^2 from tag 0 to tag +6.

In Fig 5, the physiological parameters are expressed on the NMR split scale. The same patterns for chlorophyll and starch content and can be observed in Fig. 1. By comparing conventional approaches (Fig 1) and the NMR split scale (Fig 5) it was demonstrated that the NMR split scale allowed averaging of more data for each point. Indeed, for the representation according to leaf position or leaf age (Fig. 1), number of data averaged for each point corresponded to the number of repetitions (4 in the present study). In contrast, in the case of the representation using the NMR split scale, all leaves from all plants were considered and each point represents an average of 7 to 21 measurements on individual leaves. The number of averaged data depended on the number of leaves with similar NMR signals, without taking into account the characteristics of the experimental design (leaf rank and measurement week). Moreover, the NMR split scale made it possible to extend the range of the development scale, as can be observed in Fig. 5. The NMR split scale therefore makes it possible to reconstruct the pattern of evolution of parameters throughout leaf development by taking into account all the individual leaves studied

Limb structure modifications

Changes in leaf internal structure were characterized by electronic and light micrographs. Fig. 6 represents examples of leaf light micrographs of young (tag -2), mature (tag +2) and senescing leaves (tag +4). The general structure of the leaf remained constant at all stages of leaf development, with upper epidermis, palisade parenchyma, spongy parenchyma and lower epidermis (from top to bottom). However, the tissue differentiation became trickier in senescing leaves (from tag +4) where the structure tended to be less organized. The most obvious structural modification observed between the leaf stages was the increase in leaf thickness with ageing. This was mostly due to enlargement of the palisade cells. The upper epidermis seemed to experience similar swelling to the palisade parenchyma, and the structure of the lower epidermis, that was less

affected by ageing, was likely to change in the same way. Another noticeable structural change that can be observed (Fig. 6) was the disappearance of chloroplasts during leaf development. In addition to changes in numbers of chloroplasts, plast structure was also affected by ageing. This is illustrated in Fig. 7 depicting electronic micrographs of plasts at three developmental stages. Chloroplasts had several starch granules in young and mature leaves, well defined thylakoids and few small plastoglobuli (Fig. 7a). By contrast, in gerontoplasts present in senescing leaves (Fig. 7b), plastoglobuli were larger and numerous. A few thylakoids were observed, but not stacked as in chloroplasts, and no starch granules were visible. Gerontoplasts were found mainly in senescent leaves, although a few of them were observed in mature leaves. In the final stage of development (corresponding to the oldest leaves (Fig. 7c)) plasts were constituted of relatively large lipid droplets surrounded by an envelope. These plast were not detectable by light microscopy because they were rare and because toluidine blue is known specifically to stain starch in the plast.

Changes of parenchymal structure

The structural modification of leaf tissues seen in Fig. 6 is presented in Figs. 8. The average vacuolar volume of palisade parenchyma cells increased markedly (Fig. 8), while that of spongy parenchyma remained around 0.3 mm^3. Leaf thickness increased from around 250 µm to 320 µm, mainly due to an increase in the palisade parenchyma (from 100 µm to 160 µm). The thickness of the spongy parenchyma remained at around 100 µm. Each epidermis presented a slight increase in thickness.

Note that, as mentioned earlier in Materials and Methods section, measurements of the area and width of the vacuole on the samples taken perpendicularly and parallel to the central vein confirmed that vacuole depth and width can be considered as identical, validating the model for volume estimation based on micrograph observations (Supplementary data 3).

Fig. 9 depicts the percentage of the leaf cross section occupied by each tissue according to the NMR split scale. In order to approximate vacuolar water at the tissue level, internal spaces and plasts were removed from the representation. The volume of epidermis cells represented about 15% of the leaf tissues and therefore contributed to the NMR signal. Due to their irregular shape, the volume of epidermis cells could not be estimated from micrographs. However, an increase in both upper and lower epidermis thickness was observed, indicating similar evolution of these tissues to that of palisade parenchyma, i.e. in accordance with the hydraulic designs proposed in leaves by Zwieniecki (Zwieniecki et al. 2007). We therefore supposed that the fifth component of the NMR signal reflected epidermis vacuoles in addition to the palisadic parenchyma vacuoles. In consequence, the volumes occupied by epidermis and palisade cells were pooled for comparison with NMR results (Fig. 9).

For comparison with the vacuolar water changes measured from micrographs, the percentages of the total intensity of components 4, 5 and 4+5 are represented on the same graph. The results showed an increase in volume of palisade and epidermis tissues whereas the spongy parenchyma remained constant. At the same time, the relative intensity of the fifth component increased, while that of the fourth remained almost constant. The latter indicated that the fourth component might be related to vacuoles of spongy parenchyma cells while the fifth component might correspond to those of the palisade parenchyma cells.

DISCUSSION

Differential structural changes of leaf parenchyma throughout leaf senescence

As described in the introduction, leaf parenchyma have different functions that may lead to different patterns of evolution during senescence. The major limitations for studying functions of each parenchyma separately are technical; for example, there is no easily available technique that allows differential evaluation of biochemical traits at the tissue level. In C3 plants, like oilseed rape, only structural differences between parenchyma have been analyzed in detail, due to the fact that they are visible microscopically. Microscopic studies of leaf tissue structure have mostly focused on the impact of water stress in *Arabidopsis* (Wuyts et al. 2012), peas (Martinez et al. 2007), olive trees (Bacelar et al. 2006) and horse chestnut trees (Nardini et al. 2010). The impact of ozone has also been measured at the tissue level by measuring leaf tissue thickness of different woody plant species, because of the well-known gas exchange role of spongy cells (Günthardt-Goerg et al. 2000). The results reported have shown significant differences between species in response to such stress, in terms of size and structure of parenchyma.

The different patterns of evolution of palisade and spongy cell volumes (Fig. 8) reported here could be explained by the specialized functions attributed to each type of parenchyma. In view of their major role in photosynthesis (Nardini et al. 2010), palisade cells would be more impacted by the nutrient remobilization process associated with plast dismantling, especially in terms of change in solute composition of the vacuole that is the major site of degradation of different molecules during senescence (Otegui et al. 2005). The increase in palisade cell volume corresponding to leaf hydration (Fig. 1) could be explained by cell wall loosening probably together with lowering of vacuolar osmotic potential. For instance, it has been shown on *Arabidopsis* that several cell wall degrading enzymes (β-glucosidase) are enhanced by decline in photosynthesis (Mohapatra et al. 2010), suggesting that cell wall degradation occurs in the leaf cells during senescence. These authors suggested that polysaccharides bound to the cell wall that remains intact even during the late phase of senescence may be a possible source of sugar. On the other hand, spongy cells, that have a major role in the leaf's hydraulic status (Nardini et al. 2010), are believed to regulate water status during senescence.

As a matter of fact water content was shown to increase in oilseed rape leaves during senescence (Fig. 1c and d), in accordance with findings previously reported by Musse et al. (2013). This increase is due to loss of dry weight that materializes remobilization of cell materials (Diaz et al. 2008) and to leaf hydration. This hydraulic characteristic was revealed by both micrographs and the increase in fresh weight observed during senescence progression (Supplementary data 1). The water entry is at the origin of the slight increase of the intensity of the signal corresponding to the vacuole and probably of the increase in T2. In mature leaves (tag 0), the fifth component appeared as a result of the split in the fourth component. This is supported by the fact that the sum of the LWW of two longest T2 components in mature and senescing leaves (Fig. 4) represented a continuation of the pattern of LWW of the fourth component in young leaves. After the split, the LWW and the T2 of the fourth component continue to increase slightly, and both parameters of the fifth component markedly increased. As discussed by Musse *et al*. (Musse et al. 2013), the significant increase in the T2 of the fifth component is probably due to several phenomena. First, the water influx, at the origin of cell enlargement combined with decreased dry weight, probably induced a dilution of vacuole solutes. This phenomenon was in part counterbalanced by the increase in solute concentration due to degradation processes occurring during senescence (Otegui et al. 2005). Secondly, the increase in cell volume had an impact on the T2 value because of the sensitivity of T2 to compartment size (van der Weerd et al. 2001). The trends of components 4 and 5 were

linked to the observations from the light microscopy, showing clear tissue differentiation (Figs. 8). Indeed, the vacuolar volume of the palisade cell increased markedly, whereas such changes did not occur in spongy cells. The variations in palisade vacuole volume measured in the present study (from 0.4 mm^3 (tag -2) to 1.6 mm^3 (tag 4)) affected the T2 values of the fifth component. A linear relationship between the relaxation rate (1/T2) and the sum of the inverse of the cell compartment radii has been demonstrated in maize and pearl millet by van der Weerd et al. (2001), implying constant permeability of the compartment membrane and the same solute composition of vacuole. However, the linear relationship could not be applied to the results of the present study because of the changes in the vacuole composition and because there was no evidence that tonoplast permeability did not vary during leaf development. The sudden increase in T2 of the fifth component at the very end of senescence (tag +6 and +7) and the high value of standard deviation of the measurements (Fig. 4) may be linked to active dismantling of the tonoplast of some the palisade cells just before their death. Indeed, the water enclosed in the vacuoles may then spread over the entire symplast compartment. In spongy cells the volume measured on micrograph changed very slightly during senescence compared to palisade cells and was in agreement with changes in signal intensity. The slight increase in the T2 of the fourth component was probably due to the same mechanisms in young leaves. The relatively small changes in LWW and vacuole volume in this tissue fits well with the spongy cell supposed role in the homeostasis of the leaf hydraulic status. Comparison of the relative intensity of the fourth and fifth components with the volume occupied by the two parenchyma (Fig. 9) demonstrated the attribution of the fourth component to the spongy parenchyma vacuoles and of the fifth component to the palisade parenchyma and epidermis vacuoles.

Note that several authors have postulated that leaves lose water during senescence (McIntyre 1987; Zhang et al. 2012). It was shown by Zhang *et al*. (2012) that detached senescent *Arabidopsis* leaves lose water faster than mature leaves. However, there is no abscission of the leaf in *Arabidopsis,* unlike *B. napus,* and dead leaves of *Arabidopsis* remain fastened to the plant while drying. Zhang *et al*. (2012) also showed that the abscissic acid level is greater in senescent leaves, indicating that stomata are closed. A decrease in stomatal conductance with aging has already been highlighted in *B. napus* (Albert et al. 2012). Moreover, guard cells live longer than leaf parenchyma cells (Gotow et al. 1988) and are able to control water flux in leaves until the final senescence stage.

In the present study, the focus was on the T2 components associated with the vacuole. However, certain results suggested putative attribution of the other components of the NMR signal. The third signal component of young leaves (tag -3), relaxing at about 20 ms (Fig. 4) and representing about 15% of the water signal, has previously been linked to the plasts (Musse et al. 2013). Such attribution was supported here by comparison with the results of quantitative analysis of light micrographs, showing that plasts occupied about 13% of leaf tissue volume. However, while following senescence to its final stage, as performed here, the results showed that this component was still detected when plasts had disappeared on light micrographs. Consequently, the third T2 component in senescing leaves probably originates, in addition to the plastidial water, from other proton pool relaxing at a similar relaxation rate. Several phenomena resulting from plast degradation could be at the origin of the formation of proton pools. One phenomenon may correspond to the proliferation of small vesicules such as senescent associated vacuoles (Avice and Etienne 2014; Otegui et al. 2005) and RuBisCo containing bodies (Hoertensteiner 2006). These lytic compartments have dimensions in the same order of magnitude as plasts. The second phenomenon may correspond to the proliferation and increase in size of the plastoglobuli (Brehelin et al.

2007) clearly observed on the micrographs (Fig. 3), resulting from the thylakoid membrane remobilization. Note that first and second order vascular tissues were successfully avoided by the sampling procedure; however, a few third and all fourth order vascular tissues were present in leaf samples used for NMR experiments. The contribution of these tissues to the NMR signals, and especially to the third component remains to be evaluated.

The second T2 component, relaxing at about 3 ms and representing about 2% of the water signal, has been attributed to apoplastic water and to a lesser extent to water inside starch granules (Musse et al. 2013). Our microscopy results (Supplementary data 4) are in agreement with the literature (Mohapatra et al. 2010),where it was suggested that an increase in cell wall elasticity due to its thinning can be linked to the decrease in intensity and T2 of this component just before it disappeared. Moreover the disappearance of the second component corresponded to the loss of the plast integrity, and starch granules within them.

Changes in physiological indicators of C and N remobilization throughout leaf senescence

Plasts contain 75% to 80% of total leaf nitrogen (Makino and Osmond 1991) and high amount of lipids (Thompson et al. 1998). They are thus the major source of nutrients remobilized during senescence. Plast dismantling, characterized by chlorophyll breakdown, is generally measured in terms of chlorophyll loss (BuchananWollaston 1997; Otegui et al. 2005). The chlorophyll content was shown to be constant in young and photosynthetically active leaves and to decrease slowly with ageing and plast dismantling (Ghosh et al. 2001). Our results (Fig. 1 A) are in accordance with these results and those of former studies (Inada et al. 1998; Lim et al. 2007; Otegui et al. 2005), demonstrating that the chlorophyll degradation is an early event in senescence. Chlorophyll content, as measured here, was a good indicator of the general plast status but did not make it possible to access information about specific tissues changes. This question was addressed through light microcopy. The light micrographs showed that plast degradation started with a decrease in volume and was followed by a reduction in number, in accordance with results obtained on darkened leaves (Ghosh et al. 2001; Inada et al. 1998; Keech et al. 2007). Despite the higher density of plasts observed in palisade parenchyma and the different functions attributed to leaf tissues, plast disappearance was concomitant in both parenchyma. This could indicate that the degradation mechanisms are similarly regulated.

Electron microscopy was shown to be complementary to light microscopy as it allowed the investigation of plast structure. Electron micrographs (Fig. 7) showed typical young chloroplast presenting well organized thylakoids and starch granules demonstrating plast functionality (Parthier 1988). Plastoglobuli, that are responsible for membrane replacement (Brehelin et al. 2007), were not numerous at this age. Gradual chloroplast shrinkage and transformation into gerontoplasts was clearly visible in our images (Fig. 7b) showing only a few membranes that were stacked and larger and more numerous plastoglobuli. The process described above is characterized by the disintegration and remobilization of thylakoid membranes through plastoglobuli (Thompson et al., 1998, Keech et al. 2007), leading to the accumulation of these plastoglobuli in the plast. The last stage of plast dismantling, corresponding to the oldest leaves studied (Fig. 7c), was characterized by large plastoglobuli without remaining thylakoids, surrounded by the plastidial envelope. As far as we are aware, this ultimate stage of plast dismantling has not been described in the literature to date, probably because plast evolution through senescence has mainly been studied on darkened leaves (Keech et al. 2007; Wada and Ishida

2009). Dark treatment is known to induce intracellular degradation more aggressively than natural ageing (Wada and Ishida 2009), and it probably enhanced the autophagy remobilization processes. Despite evidence of autophagy of whole plasts during senescence (Guiboileau et al. 2012; Wada and Ishida 2009), the presence of plasts at that late stage therefore demonstrated that they were not all dismantled through autophagy. This may be linked with the suboptimal nutrient remobilization observed in *Brassica napus* leaves during senescence.

Plasts contain an important part of the leaf carbon in the starch granules. Starch content (Diaz et al. 2008; Wada and Ishida 2009) is another common parameter used to monitor senescence. Masclaux et al. (2000) proposed that for tobacco leaves studied according to leaf rank, the onset of decrease in starch content represents the source/sink transition. Their results also showed a decrease in dry matter associated with remobilization during senescence. The latter phenomenon was observed in the present study (Fig. 1b and d) and was at the origin of the decrease in the intensity of the first NMR signal component, demonstrating that NMR signal could be used as indicator of remobilization activity.

While the link between tissue-specific structural modifications and efficiency of nutrient remobilization remains unknown, it is clear that the senescence-associated processes of cell enlargement and tissue hydration occurring in palisade layer may have an impact on this efficiency. Even if the cell hydration seems not to have an impact on plast disappearance, with no difference observed in terms of plast density evolution between the two parenchyma layers, one may expect differences in term of cell metabolism between the two layers that remain to be investigated.

Using parenchyma differentiation on NMR signals as a developmental marker

Investigation of leaf senescence requires knowledge of the developmental stage of the leaves studied. This stage can be determined more or less accurately via parameters such as leaf rank or leaf age, chlorophyll content, gene expression, etc. During plant development, new leaves appear at the top of the plant and leaf senescence progresses from the bottom to the top of the canopy (Masclaux et al. 2000). It should be noted that the progression of senescence is acropetal (Avice and Etienne 2014) in the leaf limb and that this phenomenon was taken into account in the sampling procedure.

In crop plants, such as oilseed rape, wheat, rice and tobacco, leaf rank scale is commonly used to present physiological results (Mae and Ohira 1981; Masclaux et al. 2000). Presentation of the results according to leaf rank and measurement week showed that leaf rank is a good criterion for monitoring natural senescence. Another approach is to tag leaves according to the time of appearance and to follow their development. If the analysis method is destructive, different plants are necessary for such analysis. However, both approaches necessitate averaging values of leaves from different plants, and are susceptible to variability because leaves from different plants of the same leaf rank or time of appearance are not necessarily of the same physiological status, even from plants grown in controlled conditions.

Chlorophyll content is also commonly used to determine physiological status as it represents a simple, non-destructive method (Otegui et al. 2005; Zhang et al. 2012). However, this method cannot be used to

discriminate between young and mature leaves with the maximum of chlorophyll. Moreover, Gombert et al. (2006) demonstrated that chlorophyll content was not a precise parameter to determine physiological status of a leaf. For instance, in the case of nitrogen deficiency, the same chlorophyll content was measured in leaves from stressed and control plants of different developmental status. Our results also showed that the method used for measurement of chlorophyll content was not suitable for determining the senescence stage of very old leaves, characterized by the absence of plasts on micrographs but still with chlorophyll content of around 10% of maximum (Fig. 5).

Similarly, starch content seems to be overvalued in old leaves. Indeed, various authors have detected small amounts of starch in old leaves where the photosynthesis apparatus has clearly been dismantled (Diaz et al. 2008; Masclaux-Daubresse et al. 2008). Our results in old leaves (tag +5 and more) also showed a small amount of starch whereas no plasts were visible on light microscopy.

Another common approach to determine the physiological status of a leaf has been to use the expression of two genes, *sag12* (*senescence associated gene 12*) that is unregulated during senescence and *cab* (*chlorophyll a/b binding protein*) that is downregulated during senescence (Gombert et al. 2006). The cross-over between in the expression of these genes was proposed as the onset of senescence. While the method is helpful to determine a specific leaf status at the cross-over, it is less clear before and after this cross-over and the method remains time consuming.

Finally, the approach using individually darkened leaves (IDL) allows control of the beginning of senescence and therefore better monitoring of plast dismantling occurring in late senescence (Keech et al. 2007). However, it may induce intracellular degradation more aggressively than natural ageing (Wada and Ishida 2009).

As described above, all the methods commonly used have specific defects. The main limitations are related to insufficient method accuracy and the limited sensitivity of the parameter selected in specific developmental ranges. In contrast, NMR signals for oilseed rape leaves were found to be very sensitive to the developmental stage over a very wide period of time. The major modification of the NMR signal is the splitting of the last T2 component of young leaves, reflecting differences in the pattern of evolution of palisade and spongy tissues. NMR measurement protocol was associated with signal analysis based on two different approaches (MEM and Levenberg-Marquardt) providing in this way a robust method for split estimation. The split appeared to be an essential stage in leaf development, and its progression in the canopy (Fig. 3) was constant (about one leaf rank per week). When using the split for tagging, the changes in the NMR signal throughout the entire development process became highly reproducible (Fig. 4). Physiological parameters occurring according to the split scale (Fig. 5) validated this approach. Moreover, the split scale allowed accurate presentation of the results over a wide range of developmental stages.

In view of the high reproducibility of the NMR signal shown in this study, it should be possible to use all the parameters in the NMR signal to identify the age of an individual leaf. As the method described is based on the differences in the pattern of evolution of palisade and spongy tissues in *Brassica napus* under specific experimental conditions, the general character of the method should be further evaluated. Indeed, this would require the acquisition of a NMR database for specific experimental conditions and other species, and would be

an important step in leaf characterization compared to current methods based on metabolic indicators (chlorophyll, starch content) that require measurement of kinetics.

CONCLUSION

In this study, different patterns of evolution of the palisade and spongy parenchyma of *Brassica napus* leaves during development were revealed, associated with leaf thickening due to cell enlargement and tissue hydration. The NMR signal was shown to be sensitive to tissue modifications, and an original interpretation was therefore proposed taking into account both cellular compartmentalization and heterogeneity at the tissue level. The experimental design of the study made it possible to follow structural and physiological changes in leaf during natural senescence, up to its ultimate stage, where late stage of gerontoplasts was revealed. The link between tissue-specific structural modifications and the efficiency of nutrient remobilization remains unknown; however, the results highlighted the importance of considering the complexity of the tissue structure while studying leaf functioning. Finally, it was also shown that the structural changes can be used instead of long-time measurements of kinetics in order to monitor leaves according to their developmental status. In the current context of fertilization reductions and climatic changes, occurrence of nitrogen depletion and water deficit is expected to increase. One interesting outcome of the present study would therefore be to see how leaf structural modifications and nutrient remobilization during senescence are impacted by these abiotic stresses.

CONFLIC OF INTEREST

The authors declare that they have no conflict of interest.

ACKNOWLEDGEMENTS

We thank the Regional Council of Bretagne for financial support. We also thank the Genetic Resources Center (BrACySol, BRC, UMR IGEPP, INRA Ploudaniel, France) for providing the seeds of the Tenor variety. We thank our colleagues of the Biopolymers, Structural Biology platform, INRA Nantes, France for their help and support with TEM studies. We thank Mireille CAMBERT (IRSTEA) for her assistance with NMR measurements, Françoise LEPRINCE for starch analysis, and Patrick LECONTE and the greenhouse team (IGEPP) for technical support with plant management.

LITERATURE CITED

Albert B, Le Caherec F, Niogret MF, Faes P, Avice JC, Leport L, Bouchereau A (2012) Nitrogen availability impacts oilseed rape (Brassica napus L.) plant water status and proline production efficiency under water-limited conditions. Planta 236: 659-676

Avice J-C, Etienne P (2014) Leaf senescence and nitrogen remobilization efficiency in oilseed rape (Brassica napus L.). Journal of experimental botany: eru177

Bacelar EA, Santos DL, Moutinho-Pereira JM, Goncalves BC, Ferreira HF, Correia CM (2006) Immediate responses and adaptative strategies of three olive cultivars under contrasting water

availability regimes: Changes on structure and chemical composition of foliage and oxidative damage. Plant Science 170: 596-605
Bohler S, Sergeant K, Jolivet Y, Hoffmann L, Hausman J-F, Dizengremel P, Renaut J (2013) A physiological and proteomic study of poplar leaves during ozone exposure combined with mild drought. Proteomics 13: 1737-1754
Brehelin C, Kessler F, van Wijk KJ (2007) Plastoglobules: versatile lipoprotein particles in plastids. Trends in Plant Science 12: 260-266
BuchananWollaston V (1997) The molecular biology of leaf senescence. Journal of Experimental Botany 48: 181-199
Capitani D, Brilli F, Mannina L, Proietti N, Loreto F (2009) In Situ Investigation of Leaf Water Status by Portable Unilateral Nuclear Magnetic Resonance. Plant Physiology 149: 1638-1647
Castro-Diez P, Puyravaud JP, Cornelissen JHC (2000) Leaf structure and anatomy as related to leaf mass per area variation in seedlings of a wide range of woody plant species and types. Oecologia 124: 476-486
Colire C, Lerumeur E, Gallier J, Decertaines J, Larher F (1988) An assessment of proton nuclear magnetic-resonance as an alternative method to describe water status of leaf tissues in wilted plants. Plant Physiology and Biochemistry 26: 767-776
Diaz C, Lemaitre T, Christ A, Azzopardi M, Kato Y, Sato F, Morot-Gaudry J-F, Le Dily F, Masclaux-Daubresse C (2008) Nitrogen recycling and remobilization are differentially controlled by leaf senescence and development stage in Arabidopsis under low nitrogen nutrition. Plant Physiology 147: 1437-1449
Ghosh S, Mahoney SR, Penterman JN, Peirson D, Dumbroff EB (2001) Ultrastructural and biochemical changes in chloroplasts during Brassica napus senescence. Plant Physiology and Biochemistry 39: 777-784
Gombert J, Etienne P, Ourry A, Le Dily F (2006) The expression patterns of SAG12/Cab genes reveal the spatial and temporal progression of leaf senescence in Brassica napus L. with sensitivity to the environment. Journal of Experimental Botany 57: 1949-1956
Gotow K, Taylor S, Zeiger E (1988) Photosynthetic carbon fixation in guard-cell protoplasts of vicia-fabia L - evidence from radiolabel experiments. Plant Physiology 86: 700-705
Guiboileau A, Yoshimoto K, Soulay F, Bataille M-P, Avice J-C, Masclaux-Daubresse C (2012) Autophagy machinery controls nitrogen remobilization at the whole-plant level under both limiting and ample nitrate conditions in Arabidopsis. The New phytologist 194: 732-740
Günthardt-Goerg M, McQuattie C, Maurer S, Frey B (2000) Visible and microscopic injury in leaves of five deciduous tree species related to current critical ozone levels. Environmental Pollution 109: 489-500
Hills BP, Remigereau B (1997) NMR studies of changes in subcellular water compartmentation in parenchyma apple tissue during drying and freezing. International Journal of Food Science and Technology 32: 51-61
Hoertensteiner S (2006) Chlorophyll degradation during senescence. Annual Review of Plant Biology, pp 55-77
Inada N, Sakai A, Kuroiwa H, Kuroiwa T (1998) Three-dimensional analysis of the senescence program in rice (Oryza sativa L.) coleoptiles - Investigations by fluorescence microscopy and electron microscopy. Planta 206: 585-597
Keech O, Pesquet E, Ahad A, Askne A, Nordvall D, Vodnala SM, Tuominen H, Hurry V, Dizengremel P, Gardestroem P (2007) The different fates of mitochondria and chloroplasts during dark-induced senescence in Arabidopsis leaves. Plant Cell and Environment 30: 1523-1534
Lim PO, Kim HJ, Nam HG (2007) Leaf senescence. Annual Review of Plant Biology, pp 115-136
Mae T, Ohira K (1981) The remobilization of Nitrogen related to leaf growth and senescence in rice *Oryza sativa* (L). Plant and Cell Physiology 22: 1067-1074
Makino A, Osmond B (1991) Effects of Nitrogen nutrition on Nitrogen partitioning between chloroplasts and mitochondria in pea and wheat. Plant Physiology 96: 355-362

Martinez JP, Silva H, Ledent JF, Pinto M (2007) Effect of drought stress on the osmotic adjustment, cell wall elasticity and cell volume of six cultivars of common beans (Phaseolus vulgaris L.). Eur. J. Agron. 26: 30-38

Masclaux-Daubresse C, Reisdorf-Cren M, Orsel M (2008) Leaf nitrogen remobilisation for plant development and grain filling. Plant Biology 10: 23-36

Masclaux C, Valadier M-H, Brugière N, Morot-Gaudry J-F, Hirel B (2000) Characterization of the sink/source transition in tobacco *Nicotiana tabacum* (L.) shoots in relation to nitrogen management and leaf senescence. Planta 211: 510-518

McCain DC (1995) Nuclear magnetic resonance study of spin relaxation and magnetic field gradients in maple leaves. Biophysical Journal 69: 1111-1116

McIntyre GI (1987) The role of water in the regulation of plant development. Canadian Journal of Botany-Revue Canadienne De Botanique 65: 1287-1298

Mohapatra PK, Patro L, Raval MK, Ramaswamy NK, Biswal UC, Biswal B (2010) Senescence-induced loss in photosynthesis enhances cell wall beta-glucosidase activity. Physiologia plantarum 138: 346-355

Musse M, De Franceschi L, Cambert M, Sorin C, Le Caherec F, Burel A, Bouchereau A, Mariette F, Leport L (2013) Structural Changes in Senescing Oilseed Rape Leaves at Tissue and Subcellular Levels Monitored by Nuclear Magnetic Resonance Relaxometry through Water Status. Plant Physiology 163: 392-406

Nardini A, Raimondo F, Lo Gullo MA, Salleo S (2010) Leafminers help us understand leaf hydraulic design. Plant Cell and Environment 33: 1091-1100

Nooden LD, Guiamet JJ, John I (1997) Senescence mechanisms. Physiologia Plantarum 101: 746-753

Oshita S, Maeda A, Kawagoe Y, Tsuchiya H, Kuroki S, Seo Y, Makino Y (2006) Change in diffusional water permeability of spinach leaf cell membrane determined by nuclear magnetic resonance relaxation time. Biosystems Engineering 95: 397-403

Otegui MS, Noh YS, Martinez DE, Vila Petroff MG, Andrew Staehelin L, Amasino RM, Guiamet JJ (2005) Senescence-associated vacuoles with intense proteolytic activity develop in leaves of Arabidopsis and soybean. Plant Journal 41: 831-844

Parthier B (1988) Gerontoplasts - the yellow end in the ontogenesis of chloroplasts. International Journal on Endocytobiosis and Cell Research 5: 163-190

Sakamoto W (2006) Protein degradation machineries in plastids. Annual Review of Plant Biology, pp 599-621

Snaar JEM, Van As H (1992a) A method for the simultaneous measurement of NMR spin-lattice and spin-spin relaxation times in compartmentalized systems. J. Magn. Reson. 99: 139-148

Snaar JEM, Van As H (1992b) Probing water compartments and membrane permeability in plant cells by 1H NMR relaxation measurements. Biophysical Journal 63: 1654-1658

Thompson JE, Froese CD, Madey E, Smith MD, Hong YW (1998) Lipid metabolism during plant senescence. Progress in Lipid Research 37: 119-141

Van As H (2007) Intact plant MRI for the study of cell water relations, membrane permeability, cell-to-cell and long distance water transport. Journal of Experimental Botany 58: 743-756

van der Weerd L, Claessens M, Ruttink T, Vergeldt FJ, Schaafsma TJ, Van As H (2001) Quantitative NMR microscopy of osmotic stress responses in maize and pearl millet. Journal of Experimental Botany 52: 2333-2343

Wada S, Ishida H (2009) Chloroplasts autophagy during senescence of individually darkened leaves. Plant signaling & behavior 4: 565-567

Wuyts N, Massonnet C, Dauzat M, Granier C (2012) Structural assessment of the impact of environmental constraints on Arabidopsis thaliana leaf growth: a 3D approach. Plant Cell and Environment 35: 1631-1646

Zhang K, Xia X, Zhang Y, Gan S-S (2012) An ABA-regulated and Golgi-localized protein phosphatase controls water loss during leaf senescence in Arabidopsis. Plant Journal 69: 667-678

Zwieniecki MA, Brodribb TJ, Holbrook NM (2007) Hydraulic design of leaves: insights from rehydration kinetics. Plant Cell and Environment 30: 910-921

Fig. 1 Changes in chlorophyll and starch content, water content and dry weight during leaf development in oilseed rape. **a**, **c** the eighth rank leaf was followed during the eight-week measurement period. **b**, **d** all leaves from four plants were analyzed at the third week of the measurement period. The values correspond to averages ± standard deviations of data collected from leaves of four individual plants

Fig. 2 Transverse relaxation time distribution (MEM) calculated from the CPMG signal for Brassica napus leaves. The dotted line represents results of the selected leaf (LR-8) obtained at four different times (weeks 1, 4, 6 and 8) of the eight-week measurement period. The solid line shows results of four leaves (LR-10, LR-7, LR-5, LR-3) from one plant at one measurement time (week 3)

Fig. 3 Leaf rank at which the longest T2 component observed in young leaves split into two components and maximum and minimum leaf ranks of the plant studied from each measurement week. Data shown are the averages (rounded to the whole number) of the four series

Fig. 4 NMR relaxation parameters of oilseed rape leaves according to the week report to the NMR split scale. Transverse relaxation times of the component 2 and 3 (**a**) and 4 and 5 (**b**) in ms and in relation to NMR split scale. **c** water distribution in the water-associated components (2-5) expressed as LWW where LWWi is specific leaf water weight of the ith signal component expressed in g m^{-2}. Values correspond to average of eight to sixteen leaves

Fig. 5 Chlorophyll content and starch content of oilseed rape leaves expressed as a percentage of the maximum in relation to the NMR split scale. Values are an average of seven to twenty-four results ± standard deviation

Fig. 6 Light micrographs of cross sections of oilseed rape leaves at three typical developmental stages: young (tag -2) (**a**), mature (tag +2) (**b**) and senescent (**c**) (tag +4). UE: upper epidermis; PP: palisade parenchyma; SP: spongy parenchyma; LE: lower epidermis

Fig. 7 Electron micrographs of plasts from oilseed rape leaves: **a** chloroplast from young (tag+2) and mature leaves; **b** gerontoplast from a senescent leaf (tag+4) and **c** plasts in final developmental stage present only in the oldest leaves (tag+5)

Fig. 8 Vacuole volume of the cells of different parenchyma of the oilseed rape leaf. Each measurement is an average of at least 40 cells of 4 different images

Fig. 9 NMR signal intensity of the fourth (white triangle) and fifth components (white square) and both components (white diamond) expressed as percentage of the total NMR signal intensity and in relation to the split. Relative volume of spongy parenchyma (black triangle) and relative volume of palisade parenchyma and epidermis (black square) measured on light micrographs of oilseed rape leaf cross-sections and presented in relation to the split and expressed as percentage of the whole limb volume. Each point represents the average of measurements from 4 to 10 images (from at least three different leaves)

figure1

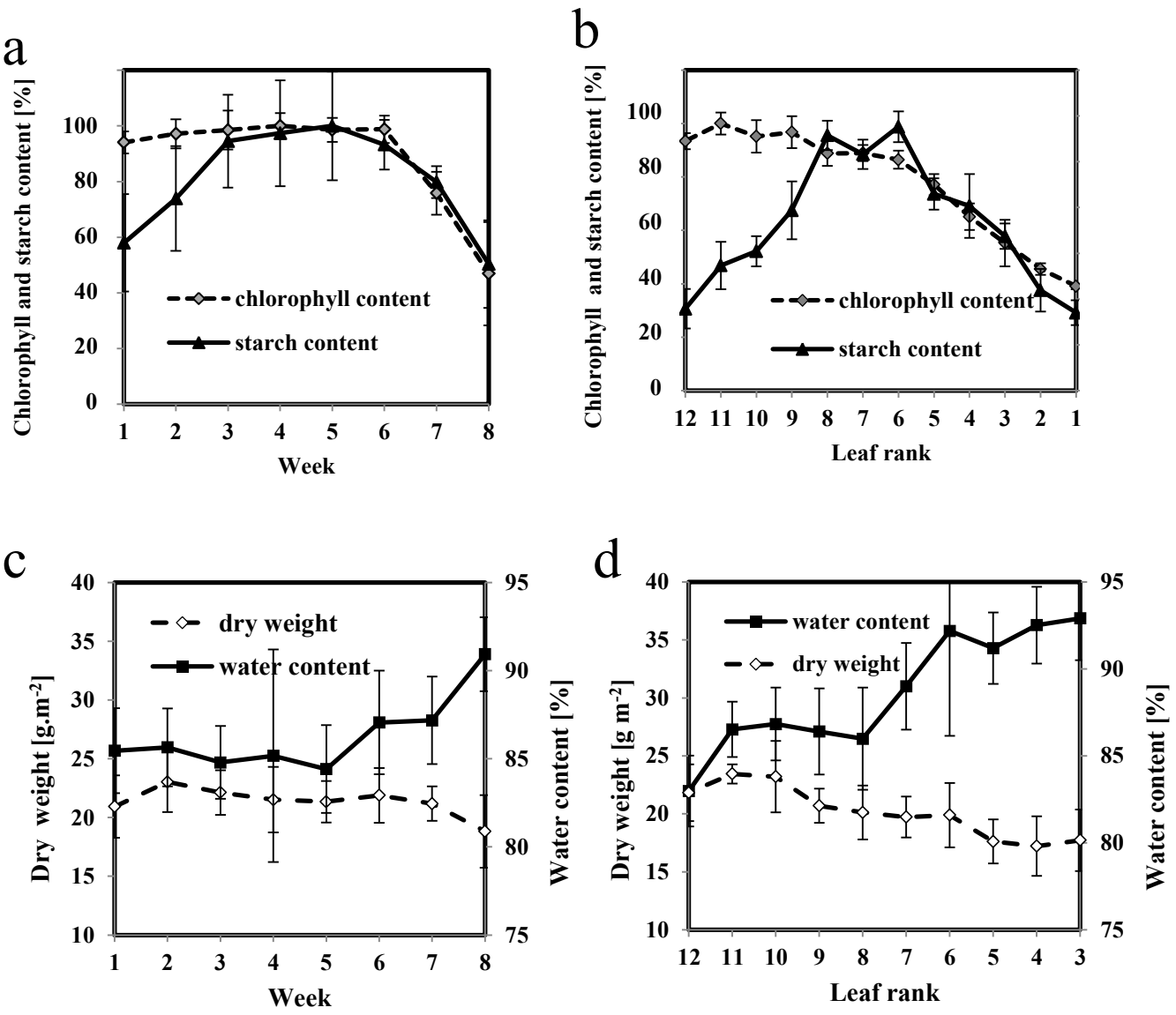

Fig. 1 Changes in chlorophyll and starch content, water content and dry weight during leaf development in oilseed rape. **a**, **c** the eighth rank leaf was followed during the eight-week measurement period. **b**, **d** all leaves from four plants were analyzed at the third week of the measurement period. The values correspond to averages ± standard deviations of data collected from leaves of four individual plants

figure2

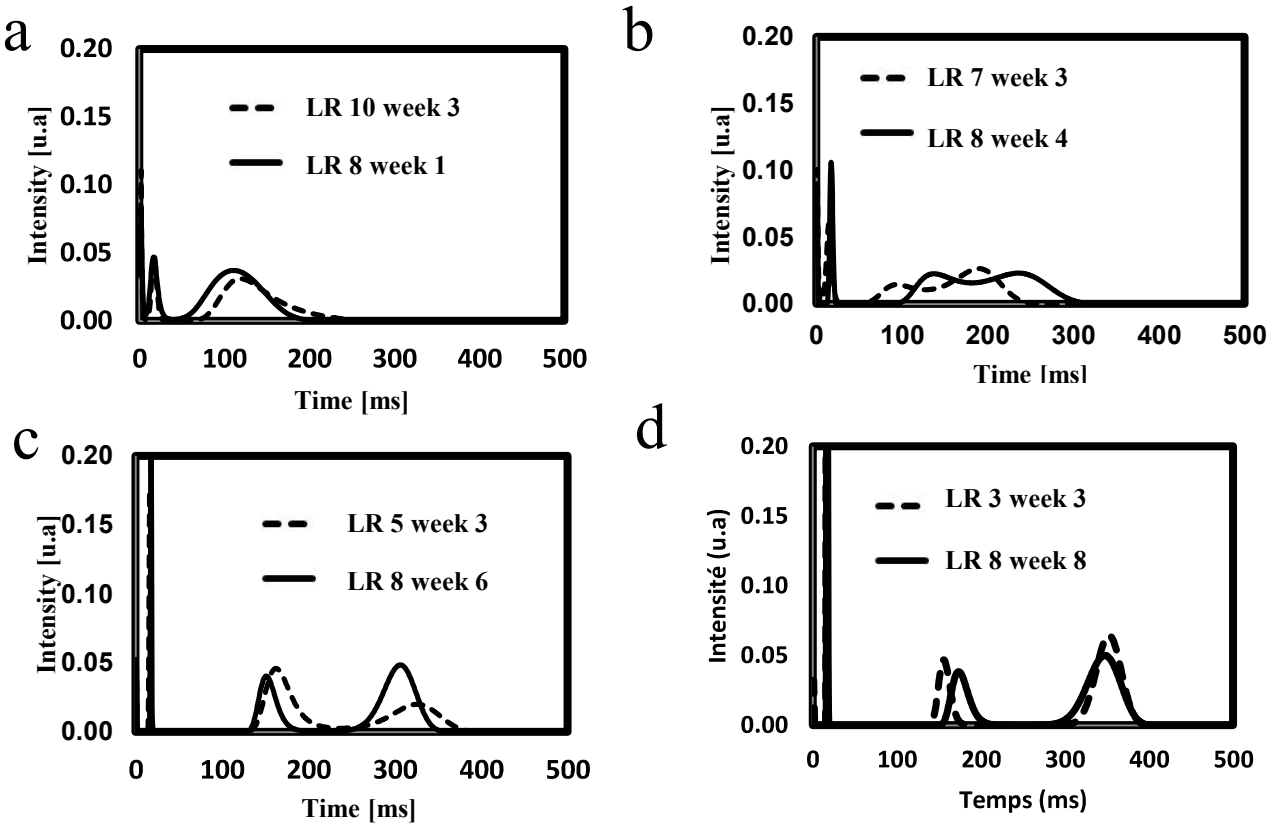

Fig. 2 Transverse relaxation time distribution (MEM) calculated from the CPMG signal for *Brassica napus* leaves. The dotted line represents results of the selected leaf (LR-8) obtained at four different times (weeks 1, 4, 6 and 8) of the eight-week measurement period. The solid line shows results of four leaves (LR-10, LR-7, LR-5, LR-3) from one plant at one measurement time (week 3)

figure3

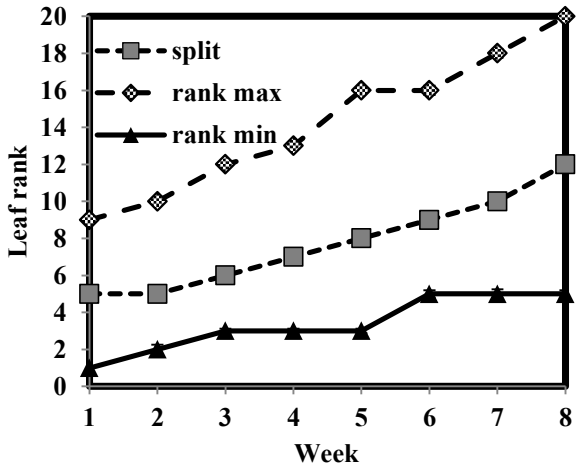

Fig. 3 Leaf rank at which the longest T2 component observed in young leaves split into two components and maximum and minimum leaf ranks of the plant studied from each measurement week. Data shown are the averages (rounded to the whole number) of the four series

figure4

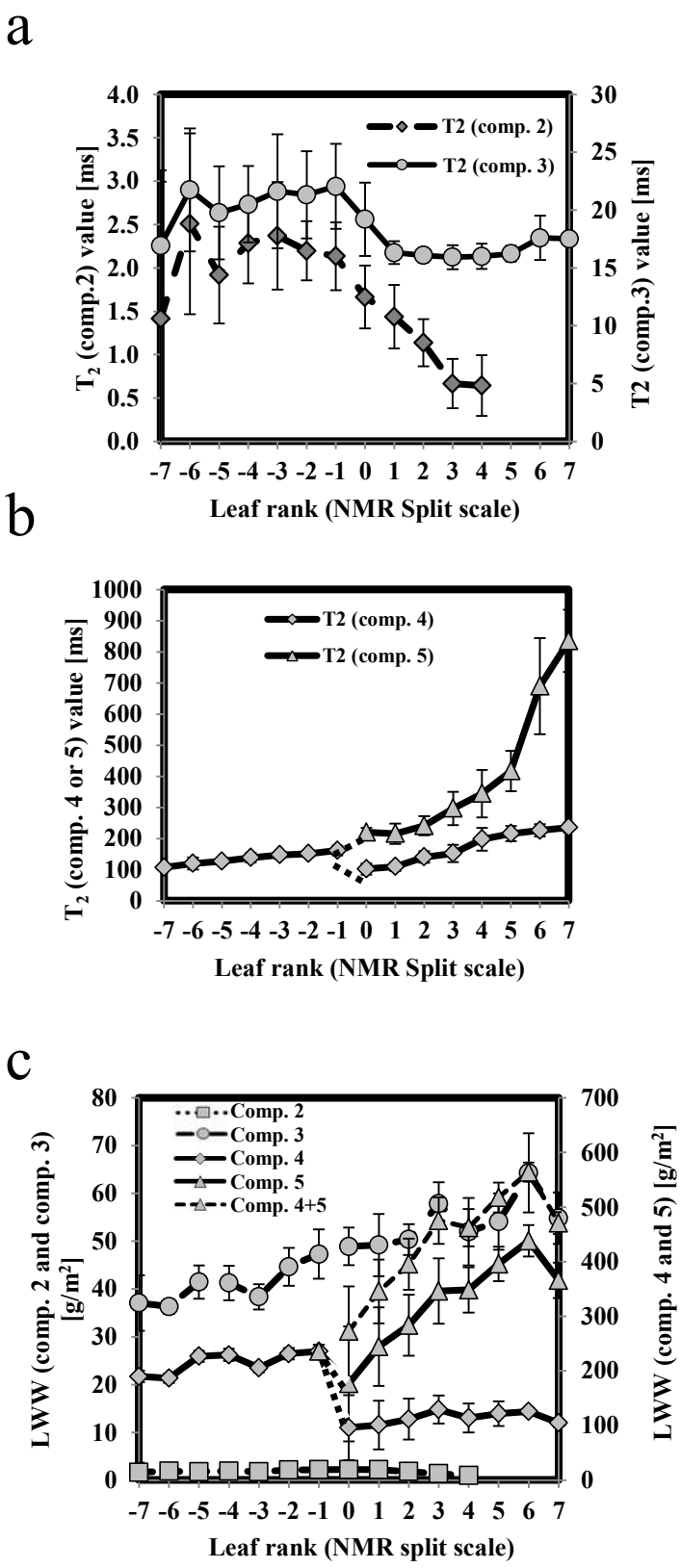

Fig. 4 NMR relaxation parameters of oilseed rape leaves according to the week report to the NMR split scale. Transverse relaxation times of the component 2 and 3 (**a**) and 4 and 5 (**b**) in ms and in relation to NMR split scale. **c** water distribution in the water-associated components (2-5) expressed as LWW where LWWi is specific leaf water weight of the ith signal component expressed in g m^{-2}. Values correspond to average of eight to sixteen leaves

figure5

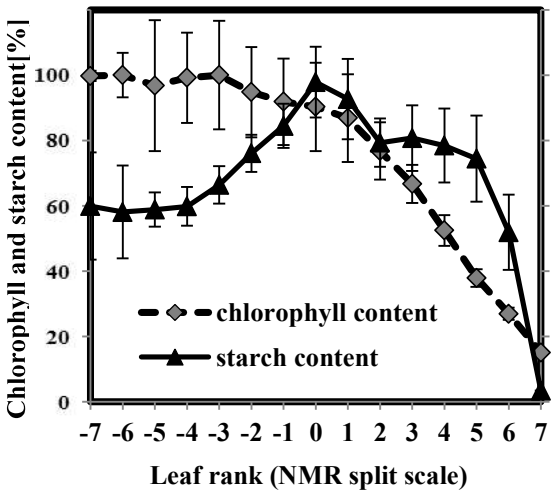

Fig. 5 Chlorophyll content and starch content of oilseed rape leaves expressed as a percentage of the maximum in relation to the NMR split scale. Values are an average of seven to twenty-four results ± standard deviation

figure6

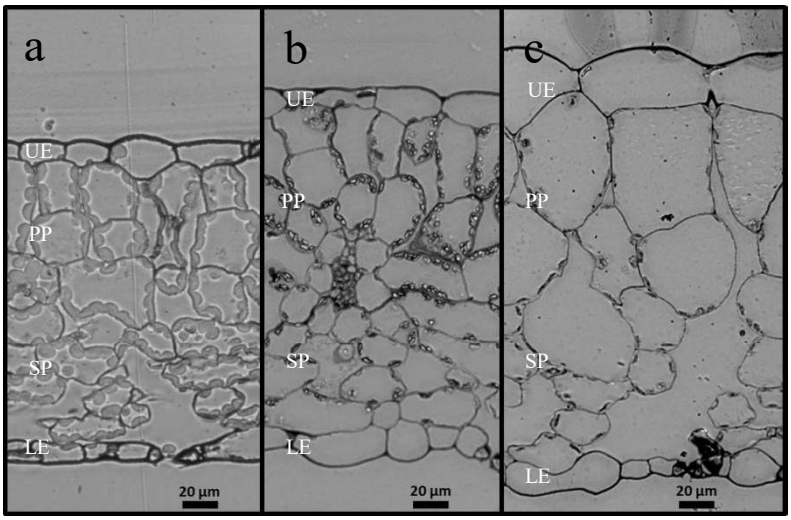

Fig. 6 Light micrographs of cross sections of oilseed rape leaves at three typical developmental stages: young (tag -2) (**a**), mature (tag +2) (**b**) and senescent (**c**) (tag +4). UE: upper epidermis; PP: palisade parenchyma; SP: spongy parenchyma; LE: lower epidermis

figure7

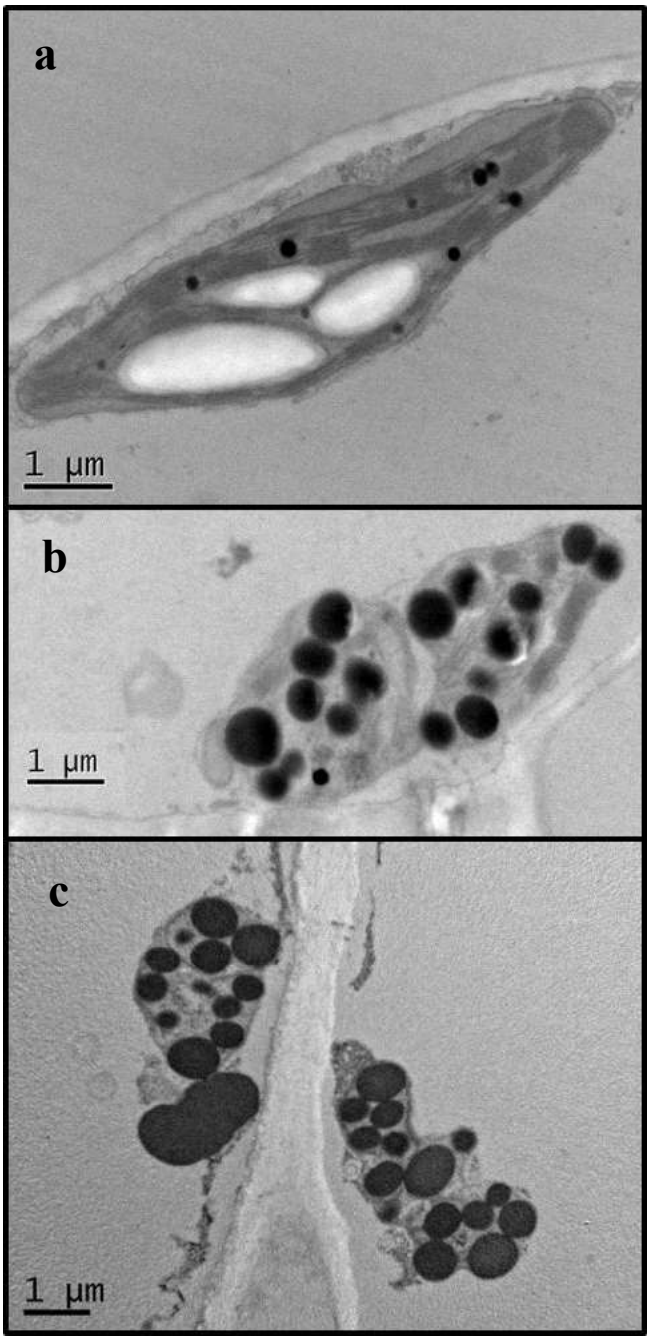

Fig. 7 Electron micrographs of plasts from oilseed rape leaves: **a** chloroplast from young (tag+2) and mature leaves; **b** gerontoplast from a senescent leaf (tag+4) and **c** plasts in final developmental stage present only in the oldest leaves (tag+5)

figure8

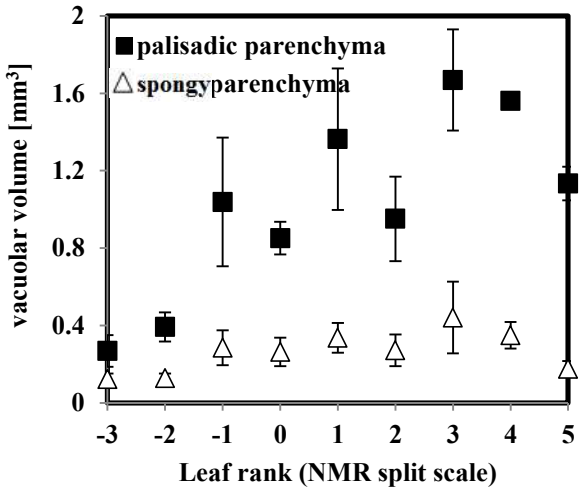

Fig. 8 Vacuole volume of the cells of different parenchyma of the oilseed rape leaf. Each measurement is an average of at least 40 cells of 4 different images

figure9

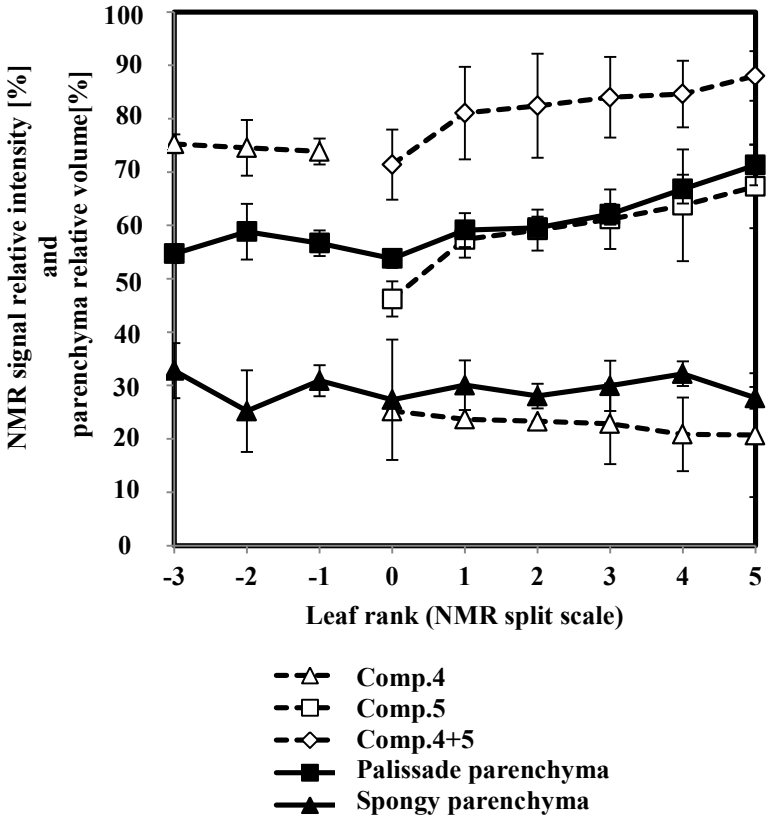

Fig. 9 NMR signal intensity of the fourth (white triangle) and fifth components (white square) and both components (white diamond) expressed as percentage of the total NMR signal intensity and in relation to the split. Relative volume of spongy parenchyma (black triangle) and relative volume of palisade parenchyma and epidermis (black square) measured on light micrographs of oilseed rape leaf cross-sections and presented in relation to the split and expressed as percentage of the whole limb volume. Each point represents the average of measurements from 4 to 10 images (from at least three different leaves)